Magnetic, thermal, and transport properties of $Fe_{100-x}V_x$ and $(Fe_{100-x}V_x)_{83}B_{17}$ alloys

S. U. Jen and S. A. Chang
Institute of Physics, Academia Sinica, Taipei, Taiwan 11529, Republic of China
(Received 21 August 1992)

Polycrystalline $Fe_{100-x}V_x$ with $x=1.2$–25 at. % and amorphous $(Fe_{100-x}V_x)_{83}B_{17}$ with $x=0$–19.3 at. % were prepared. The physical properties measured for these samples included the magnetic moment, the high-field susceptibility, the specific heat, the residual resistivity, and the anisotropic magnetoresistance at low temperatures. We have now more experimental data for $Fe_{100-x}V_x$ alloys to test the prediction of the split-band model. As to $(Fe_{100-x}V_x)_{83}B_{17}$ alloys, the complications of the spin-glass property and the strong increase of resistivity due to *s-s* scattering make the test very difficult. However, the existence of a maximum in the high-field susceptibility in $(Fe_{94.2}V_{5.8})_{83}B_{17}$ indicates a near degeneracy at the Fermi level, which may or may not be associated with the split-band model.

I. INTRODUCTION

It is well known that the split-band model[1] is applicable to polycrystalline $Fe_{100-x}V_x$ alloys,[2] because the valence difference Z between Fe and V is larger than 2. Therefore, as the Fermi level ε_F passes through the boundary (T) between the iron and the vanadium subbands, some anomalous phenomena, like the electronic specific-heat coefficient γ_{el} going through a minimum, and the anisotropic magnetoresistance $\Delta\rho/\rho_0$ going through a maximum,[2] are theoretically predicted and are experimentally observed.

In this paper, we shall focus on the discussion of the applicability of the split-band model to the amorphous $(Fe_{100-x}V_x)_{83}B_{17}$ alloys. Hence, the saturation magnetization, the high-field susceptibility χ_{HF}, the specific-heat coefficient γ, the residual resistivity ρ_0, and the anisotropic magnetoresistance $\Delta\rho/\rho_0$ data are presented for $Fe_{100-x}V_x$ as well as $(Fe_{100-x}V_x)_{83}B_{17}$ alloys to make comparisons possible. In doing so, we not only gathered more evidences for the split-band model for $Fe_{100-x}V_x$ alloys, but also obtained new experimental results for $(Fe_{100-x}V_x)_{83}B_{17}$ alloys. Unfortunately, because of the complications of the spin-glass phenomena in the latter alloys with $x \geq 6$–8, the analysis becomes more difficult. Nevertheless, our analysis from the viewpoint of the split-band model is worthwhile, and it can be extended to other iron-based alloys (crystalline or amorphous).

In the past, several authors[3–5] have attempted to explain the $\Delta\rho/\rho_0$ data in some (Fe-Ni)-based amorphous alloys by invoking ferromagnetic weakness. Hence, experimentally speaking, the trend of $\Delta\rho/\rho_0$ as a function of x is often connected with that of magnetization. In our case also, this is true. However, besides the $\Delta\rho/\rho_0$ and the magnetization data, we also have the γ and the χ_{HF} data. Therefore, additional information (including some theoretical models) will help us to understand further these amorphous alloys. In general, it is assumed that (i) the charge-transfer model[6–8] can be applied to magnetization data shown later in $(Fe_{100-x}V_x)_{83}B_{17}$ alloys, and (ii) the Fermi level ϵ_F is pinned in the middle valley of the spin-down $3d$ band[2] [i.e., $D_\downarrow(\epsilon_F) \sim$ const.].

Then we will see that not all the $(Fe\text{-}V)_{83}B_{17}$ data contradict the predictions from the split-band model. The high-field susceptibility χ_{HF} data seem to be in accordance with the model. Whether this is a concrete evidence for the split-band model in the amorphous alloys or not is discussed in details later.

II. EXPERIMENTAL DETAILS

High-purity (Puratronic grade) Fe and V, and medium-purity (99.9%) B elements were purchased from Johnson-Matthey, Co. to make polycrystalline $Fe_{100-x}V_x$ ($x=1.2$, 3.5, 6.0, 8.5, 12, 20, and 25 at. %) and amorphous $(Fe_{100-x}V_x)_{83}B_{17}$ ($x=0$, 1.9, 5.8, 11.5, and 19.3 at. %) alloys. An arc furnace was used to melt the proper constituents in a high-purity argon atmosphere. Each ingot weighs 3 g for Fe-V and 5 g for $(Fe\text{-}V)_{83}B_{17}$ alloys, and has been remelted several times to increase homogeneity. Since usually the weight loss in Fe-V alloys is very small, we take the nominal compositions to be the actual ones. For $(Fe\text{-}V)_{83}B_{17}$ alloys, due to slightly higher loss of boron, we have done atomic emission spectroscopic (AES) analysis. Then the compositions quoted above for $(Fe\text{-}V)_{83}B_{17}$ alloys are the analyzed values.

In the case of Fe-V alloys, samples were cut into the shape of rectangular plates, and then annealed at 900 °C in high vacuum for 1 h.

For making the amorphous $(Fe\text{-}V)_{83}B_{17}$ alloys, a melt spinner was utilized. To prevent oxidation, the whole apparatus is encased in a vacuum chamber. The quenching operation was carried out in an argon atmosphere. The speed of the copper wheel at the rim is about 30 m/s. The ribbon width is in the range 1–2 mm. The amorphous state of the sample was checked with an x-ray diffractometer. The thickness of the ribbons was measured by observing its cross section in the SEM. For $Fe_{83}B_{17}$, the averaged measured thickness agrees roughly with that calculated from the density and the weight of the sample. We used the measured thickness to calculate the electrical resistivity of the sample.

The magnetic moment measurements were performed in a SQUID magnetometer at 5 K. External fields H were parallel to the longer axis of the sample. The magnitudes of the fields range from 2–5 T. According to the law of approach to saturation,[9] the measured moment σ is

$$\sigma=\sigma_s\left[1-\frac{a}{H}-\frac{b}{H^2}\right]+\chi_{\mathrm{HF}}H\ , \tag{1}$$

where σ_s is the saturation moment, χ_{HF} is the high-field susceptibility, a is related to defects in the sample, and b is proportional to the anisotropy energy K_u. Because (i) the number of defects in an annealed or amorphous sample is usually small, and (ii) our samples are all very soft, it is assumed that a and b are negligible. Then, by plotting σ versus H, we obtain a fairly linear curve. From the slope and the intercept, χ_{HF} and σ_s can be determined, respectively. The number n_B of the Bohr magneton is calculated from σ_s and the molecular weight. For the amorphous samples, it is expressed as n_B per unit transition-metal atom (n_B/TM).

For the specific-heat measurements, we used the thermal relaxation method.[10] This method has the advantage of measuring the specific heat C of tiny samples with masses of 10–50 mg. On one side of the sapphire sample holder, there are a carbon glass thermometer and a nichrome thin-film heater. On the other side, the sample's flat face is in contact with that of the holder. For the amorphous samples, several pieces are stacked together and N Grease is used to enhance the thermal conduction between the pieces. Next, the whole sample holder is connected to the mount by six fine gold wires whose thermal conductivity is K. While the heater power P_0 is on, from the steady-state temperature gradient ΔT, we calculate $K=P_0/\Delta T$. After switching off the heater and letting the system relax, the time constant $\tau=C_T/K$, where C_T is the total heat capacity of the sample and the addendum. The temperature range of measurements is between 2 and 5 K. For every 0.1–0.2 K, a specific-heat datum is taken. Since the specific heat of the addendum can be measured separately, C of the sample is separated out and plotted against T, or C/T versus T^2. In the latter plot, the linear fit is somewhat good. From the intercept, we obtain the value for γ. If at low temperatures the sample is in a spin-glass state,[11] the general expression for γ is

$$\gamma=\gamma_{\mathrm{el}}+\gamma_{\mathrm{spin}}\ , \tag{2}$$

where γ_{el} is the electronic component and γ_{spin} is the spin-glass component.

To make a calibration we have chosen a pure Al sample and measured its specific heat. The γ_{el} of Al was found to be 1.41×10^{-3} J/mole K^2, which is in close agreement with the standard value.[12]

For the transport properties, we have measured the electrical resistivity ρ_0 in zero field, and the anisotropic magnetoresistance $\Delta\rho/\rho_0$ at 4 K. A dc current and a four-probe method were used to measure the electrical resistivity. The sample was mounted on the cold head of a CF1200 liquid-helium cryostat, made by Oxford Instruments. External fields up to 1 T were provided from a 7-in. electromagnet. The sample is aligned either parallel or perpendicular to the field to measure $\rho_\parallel$ and $\rho_\perp$. $\Delta\rho/\rho_0$ is defined as $\Delta\rho/\rho_0=(\rho_\parallel^s-\rho_\perp^s)/(2/3\rho_\perp^s+1/3\rho_\parallel^s)$, where $\rho_\parallel^s$ and $\rho_\perp^s$ are the saturated resistivities of $\rho_\parallel$ and $\rho_\perp$.

III. RESULTS AND DISCUSSION

Before presenting the experimental data, let us see what the split-band and the charge-transfer models predict for amorphous $(\mathrm{Fe\text{-}V})_{83}\mathrm{B}_{17}$ alloys. In the case of Fe-V alloys, it is known that the equivalent expression for the boundary T in terms of the vanadium atomic concentration x_T is governed by the equation[2]

$$5x_T=0.3-Zx_T\ . \tag{3}$$

Then, according to the charge-transfer model for amorphous alloys, each boron atom is found to contribute an average of 2.4 to 1.6 electrons to the TM $3d$ bands.[4,7] Since there are 17% of boron, the total average number of electrons transferred is 0.34. Then, from $\delta n_e^{\uparrow}+\delta n_e^{\downarrow}=0.34$ and $\delta n_e^{\downarrow}-\delta n_e^{\uparrow}=0.2$, where $\delta n_e^{\downarrow}$ is the number of electrons transferred to spin-down band, and $\delta n_e^{\uparrow}$ is that to spin-up band, it is easy to show $\delta n_e^{\downarrow}=0.27$ and $\delta n_e^{\uparrow}=0.07$. Hence Eq. (1) is modified as

$$5x_T^a=0.3-Zx_T^a-0.07\ . \tag{4}$$

Equation (4) is solved to give $x_T^a\simeq 11.5$ at. %. This means that, if the addition of boron and the formation of amorphous phase only make a simple charge-transfer effect, the boundary T is shifted to the left of $x_T=15$ at. %. We would also, in principle, observe similar anomalous phenomena in $(\mathrm{Fe\text{-}V})_{83}\mathrm{B}_{17}$ alloys at $x\simeq x_T^a$.

Figure 1 shows the magnetization data of Fe-V and $(\mathrm{Fe\text{-}V})_{83}\mathrm{B}_{17}$ alloys. Since the relation between electron per atom (e/a) and x is linear, we see clearly that the Fe-V data follow the Slater-Pauling curve,[13] with a decrease of moment of $1\mu_B$ per e/a. The functional dependence of n_B/TM for $(\mathrm{Fe\text{-}V})_{83}\mathrm{B}_{17}$ can be separated into

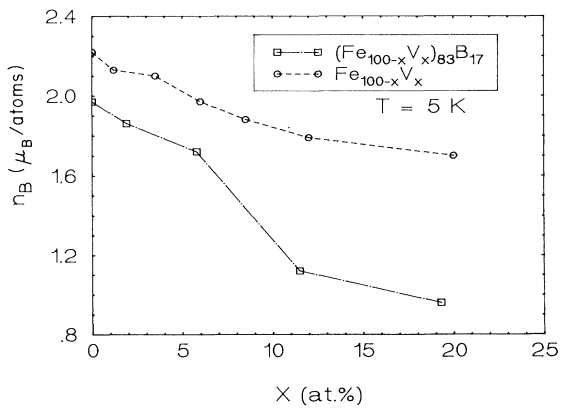

FIG. 1. The atomic magnetic moment (number of Bohr magneton n_B or n_B per transition elements) of $\mathrm{Fe}_{100-x}\mathrm{V}_x$ and $(\mathrm{Fe}_{100-x}\mathrm{V}_x)_{83}\mathrm{B}_{17}$ alloys as a function of x at $T=5$ K.

two linear regions: When $x > 5.8$ at. %, the ground state of $(Fe\text{-}V)_{83}B_{17}$ is a spin-glass state. Hence, there is a sudden downward deviation of n_B/TM around $x = 5.8$ at. %. This is due to the onset of the antiferromagnetic interaction. When $x \leq 5.8$ at. %, the parallelism between the Fe-V data and the $(Fe\text{-}V)_{83}B_{17}$ data indicates that indeed the charge-transfer model can be applied to the ferromagnetic $(Fe\text{-}V)_{83}B_{17}$ alloys. Note, the decrease of n_B from Fe to $Fe_{83}B_{17}$ in Fig. 1 is $0.27-0.07=0.2\mu_B$ as discussed.

In Fig. 2, the γ values of Fe-V and $(Fe\text{-}V)_{83}B_{17}$ are plotted together as a function of x. As predicted before, the γ_{el} of Fe-V has a minimum around $x = 10$ at. %, which is close to the value of x_T stated above. Because $D_\downarrow(\epsilon_F) \sim$ const., the relation $\gamma_{el} \propto (1+\lambda)[D_\uparrow(\epsilon_F) + D_\downarrow(\epsilon_F)]$, where λ is the electron-phonon enhancement factor, and $D_\uparrow(\epsilon_F)$ and $D_\downarrow(\epsilon_F)$ are the densities of states at the Fermi level for the spin-up and spin-down $3d$ bands, can be reduced to $\gamma_{el} \propto (1+\lambda)[D_\uparrow(\epsilon_F)]$. Therefore, γ_{el} of Fe-V tracks its spin-up $3d$ band closely, and the boundary T exists.

For the amorphous $(Fe\text{-}V)_{83}B_{17}$ alloys, the situation becomes complicated. First, it is noticed that when $x \geq 1.9$ at. %, γ of $(Fe\text{-}V)_{83}B_{17}$ increases sharply. This is due to the spin-glass contribution which covers up the electronic term γ_{el} in Eq. (2). Hence, it is difficult to find any minimum of γ_{el} in the amorphous counterpart. All that can be said is that from $x = 0$ to $x = 1.9$ at. % of $(Fe\text{-}V)_{83}B_{17}$, the γ_{el} stays constant. Moreover, in this limited x range, γ_{el} of $(Fe\text{-}V)_{83}B_{17}$ is about 1.6 times that of Fe-V. This does not mean that $D_\uparrow(\epsilon_F)$ of Fe-V is lower than that of $(Fe\text{-}V)_{83}B_{17}$. On the contrary, from the x-ray photoemission spectroscopy (XPS),[14] it is known that $D(\epsilon_F)$ of amorphous $Fe_{84}B_{16}$ is lower than that of pure Fe. The reason may be manifold. The theory of Nagel and Tauc[15] states that it is a structure-induced effect. However, since their theory is based on the nearly-free-electron model, one is not sure if it can be extended to d-state electrons. Here we interpret it as a fact that because the λ factor in amorphous materials is about three to nine times larger than that in crystalline counterparts, the strong electron-phonon scatterings may blur the Fermi surface and change the shapes of the d bands. Similarly, the Heisenberg uncertainty principle $l\Delta\mathcal{R}_F \simeq 1$ shows that the shorter the electron mean free path l through electron-phonon scatterings, the larger is the blurring $\Delta\mathcal{R}_F$ of the Fermi surface. Then, (i) the reduction of $D(\epsilon_F)$, and (ii) the smearing of $D(\epsilon_F)$ from the fact that the low- or high-temperature thermoelectric power $\simeq (dD/d\epsilon)_{\epsilon_F}$ is smaller in the amorphous case imply that the bandwidth W of amorphous $(Fe\text{-}V)_{83}B_{17}$ becomes wider than that of Fe-V (Appendix A). The split-band criterion,[1] $|\epsilon_{Fe} - \epsilon_V| > W$, where ϵ_{Fe} and ϵ_V are the nuclear electrostatic energies of electrons at Fe and V sites, respectively, is less satisfied for $(Fe\text{-}V)_{83}B_{17}$. In other words, the broadening of Fe and V bands will make instead a more common band in the amorphous alloys. The minimum in γ_{el} of $(Fe\text{-}V)_{83}B_{17}$, if it existed, would be a very shallow one.

Figure 3 shows the normalized high-field susceptibility χ_{HF}/χ^0_{HF} data of Fe-V and $(Fe\text{-}V)_{83}B_{17}$ plotted against vanadium concentration x. χ^0_{HF} is the χ_{HF} value at $x = 0$. The two measured values of χ^0_{HF} in Fig. 3 agree well with those from the literature.[4,12] The x dependence of χ_{HF}/χ^0_{HF} of Fe-V is similar to that of $(Fe\text{-}V)_{83}B_{17}$, i.e., there is a maximum in χ_{HF}/χ^0_{HF} at $x = 12$ at. % for Fe-V, and a maximum of $x = 5.8$ at. % for $(F\text{-}V)_{83}B_{17}$. This maximal behavior in χ_{HF} can be related to that in the forced magnetoresistivity $(1/\rho)(d\rho/dH)$ above saturation of Fe-V alloys.[2,16] In general, $(1/\rho)(d\rho/dH)$ can be expressed as the sum of $[(1/\rho)(d\rho/dH)]_{mag}$ due to electron-magnon scattering, and $[(1/\rho)(d\rho/dH)]_\chi \propto \chi_{HF}$.[17] The first term is negative, and the second is positive. Since there is a maximum of $[(1/\rho)(d\rho/dH)]_\chi$ due to χ_{HF} and $[(1/\rho)(d\rho/dH)]_{mag}$ is roughly the same for all x, it is easy to obtain the x dependence of $(1/\rho)(d\rho/dH)$ as in Fig. 2 of Refs. 2 and 16.

Here we discuss the origin of the maximum in χ_{HF} observed for both series of samples. In ferromagnetic met-

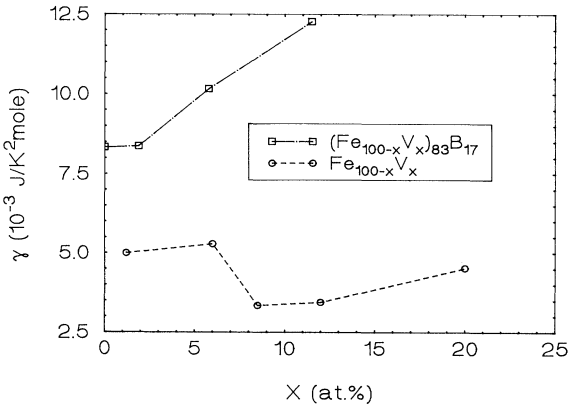

FIG. 2. The specific-heat coefficient γ as a function of vanadium concentration x for $Fe_{100-x}V_x$ and $(Fe_{100-x}V_x)_{83}B_{17}$ alloys. γ is defined from the specific heat $C = \gamma T + AT^3$.

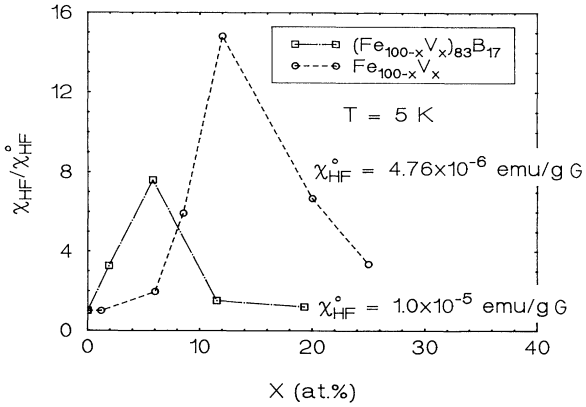

FIG. 3. The normalized high-field susceptibility χ_{HF}/χ^0_{HF} plotted vs vanadium concentration x for $Fe_{100-x}V_x$ and $(Fe_{100-x}V_x)_{83}B_{17}$ alloys at $T = 5$ K. χ^0_{HF} is the χ_{HF} value at $x = 0$.

als, χ_{HF} is expressed as

$$\chi_{HF}=\chi_s+\chi_{orb}+\chi_d \ , \tag{5}$$

where χ_s is the Pauli spin term, χ_{orb} is the orbital term, and χ_d is the Landau diamagnetic term. For Fe-rich alloys, $\chi_s+\chi_{orb}\gg|\chi_d|$.[18] Hence, we may neglect the χ_d term in Eq. (5). Then, the possible contribution to the maxima in χ_{HF} may come from either χ_s or χ_{orb}. To separate χ_s and χ_{orb}, we need the Knight shift data which are lacking. The following argument is given. From the itinerant ferromagnetic theory,[19] it is shown that

$$\chi_s=\frac{4\mu_B^2}{[D_\uparrow(\epsilon_F)]^{-1}+[D_\downarrow(\epsilon_F)]^{-1}+W_{ex}} \ , \tag{6}$$

where W_{ex} is a measure of the exchange energy. Since in Fe-rich alloys, $D_\uparrow(\epsilon_F)\gg D_\downarrow(\epsilon_F)$, we may simplify Eq. (6) as $\chi_s\propto D_\downarrow(\epsilon_F)$. In general, the relation $[D_\downarrow(\epsilon_F)]^{-1}>W_{ex}>[D_\uparrow(\epsilon_F)]^{-1}$ is satisfied. Then, the pinning of the Fermi level in the spin-down $3d$ band implies that $\chi_s\sim D_\downarrow(\epsilon_F)\sim$const. This result seems to have ruled out the possibility of the maximal contribution to χ_{HF} from χ_s.

As to χ_{orb}, the formula shows that[20]

$$\chi_{orb}\propto\sum_{nn'}\int\frac{d\mathcal{R}}{(2\pi)^3}\frac{f(E_n(\mathcal{R}))-f(E_{n'}(\mathcal{R}))}{E_n-E_{n'}}\times|\langle n|L_z|n'\rangle|^2 \ , \tag{7}$$

where $\mathcal{R}$ is the wave vector, L_z is the z component of the orbital momentum, $f(E_n)$ is the Fermi distribution, and E_n is the energy of state $n(\mathcal{R})$. To simplify Eq. (7), the term $f(E_n)-f(E_{n'})$ in the summation is equivalent to $n_e(5-n_e)$,[21] where n_e and $(5-n_e)$ are the numbers of occupied and unoccupied states in the spin-up $3d$ band respectively. Here we have considered that each spin-band contributes independently to χ_{orb}, and the contribution from the spin-up $3d$ band dominates. Then, Eq. (7) can be written as

$$\chi_{orb}\propto n_e(5-n_e)\frac{|\langle n|L_z|n'\rangle|^2}{E_n(\mathcal{R}_F)-E_{n'}(\mathcal{R}_F)} \ , \tag{8}$$

where $\mathcal{R}_F$ is the Fermi wave vector. In other words, if the band is either completely full or completely empty, there is no χ_{orb}, as shown in Fig. 4. The term $[\langle n|L_z|n'\rangle]^2/(E_n-E_{n'})$ in Eq. (8) is an implicit function of n_e through $\mathcal{R}_F$. Equation (8) and Fig. 4 mean that as the Fermi level moves from the iron subband to the vanadium subband (i.e., as n_e or x changes), only one term at $\mathcal{R}=\mathcal{R}_F$ is considered. All the other terms for $\mathcal{R}<\mathcal{R}_F$ are neglected. Also, if E_n is the energy of an occupied state, $E_{n'}$ is that of an unoccupied state. From Ref. 22, it is assumed that as ϵ_F passes through a near degeneracy, n_e goes through the magic number. Then, because of this small splitting of degeneracy at $\mathcal{R}_F$, the $(E_n-E_{n'})$ term in the denominator will give a maximal contribution to χ_{orb}. At the same time the term $\langle n|L_z|n'\rangle$ does not become zero as the term $\langle n|L_z|m\rangle$ does in the split-band calculations,[1] because here we consider the occupied n and unoccupied n' pair, instead of all the (n,m) pairs, at ϵ_F. However, because the later version of the split-band theory did not mention the degeneracy, one is not certain whether this is a necessary condition for the boundary T or not. Another indication from Fig. 4 is that due to the $[\langle n|L_z|n'\rangle]^2/(E_n-E_{n'})$ term, the maximum of χ_{orb} is shifted from the center ($n_e=2.5$) to the boundary T (where $n_e\simeq4.3$). This is exactly what is observed experimentally in Fig. 3. The more interesting point is that our previous prediction of x_T^a being at the left of x_T is also reflected in Fig. 3. Finally, we emphasize that by invoking the splitting of degeneracy, we have already inferred the intraband L_zS_z mechanism in the spin-up band.

The residual resistivities ρ_0 of Fe-V and $(Fe\text{-}V)_{83}B_{17}$ are shown in Fig. 5. As usual, ρ_0 of the amorphous phase is much larger ($\sim$25 times) than that of the crystalline phase. Obviously, the structural disorder and the metalloid impurity have strongly disturbed the scattering potential, and ρ_0 increases dramatically. This indicates that the resistivity due to s-s scattering, ρ_{ss}, becomes larger

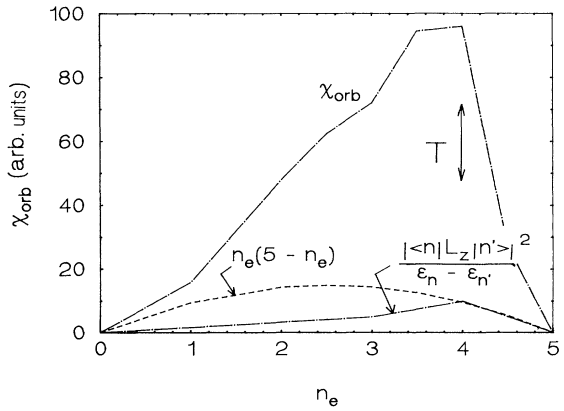

FIG. 4. The simple model representation of the orbital susceptibility χ_{orb} as a function of the number of spin-up $3d$ electrons n_e. $\chi_{orb}\propto n_e(5-n_e)[|\langle n|L_z|n'\rangle|^2/(E_n-E_n')]$. E_n and E_n' are the energies of the occupied and unoccupied states, respectively.

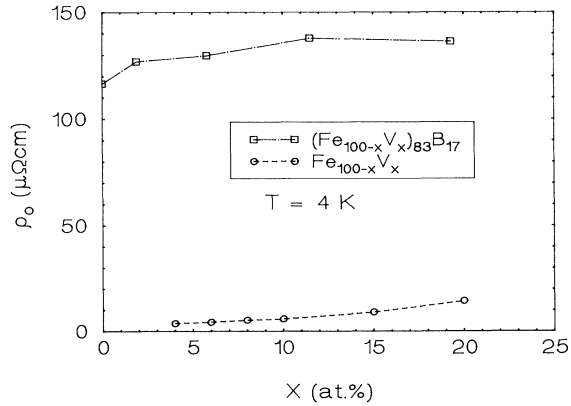

FIG. 5. The residual resistivity ρ_0 of $Fe_{100-x}V_x$ and $(Fe_{100-x}V_x)_{83}B_{17}$ alloys plotted against vanadium concentration x at $T=4$ K.

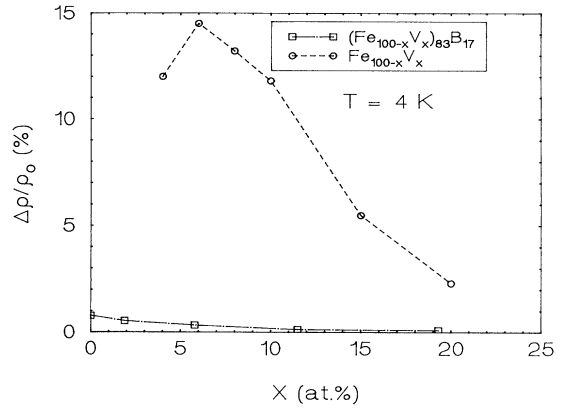

FIG. 6. The anisotropic magnetoresistance $\Delta\rho/\rho_0$ of $Fe_{100-x}V_x$ and $(Fe_{100-x}V_x)_{83}B_{17}$ alloys as a function of vanadium concentration x at $T=4$ K.

than or comparable to that due to s-d scattering, ρ_{sd}.[3] Because of this complication, we do not analyze ρ_0 of amorphous $(Fe\text{-}V)_{83}B_{17}$ here. As to the Fe-V alloys, because the spin-up resistivity $\rho_\uparrow$ is much larger than the spin-down resistivity $\rho_\downarrow$, the two-current model,[23] $\rho_0^{-1}=\rho_\downarrow^{-1}+\rho_\uparrow^{-1}$, implies that $\rho_0\simeq\rho_\downarrow$. Since $\rho_\downarrow\propto D_\downarrow(\epsilon_F)$ and ρ_0 of $Fe_{100-x}V_x$ with $0<x<15$ in Fig. 5 is constant, these imply that indeed $D_\downarrow(\epsilon_F)$ is a constant as stated before.

Figure 6 shows the anisotropic magnetoresistance $\Delta\rho/\rho_0$ of Fe-V and $(Fe\text{-}V)_{83}B_{17}$ at 4 K. As already known, for Fe-V alloys, $\Delta\rho/\rho_0$ peaks at $x\cong 6$ at. %, and $\rho_\uparrow$ peaks at $x\cong 10$ at. %. It adds proof to the existence of the boundary T in Fe-V alloys. However, the situation is different for amorphous $(Fe\text{-}V)_{83}B_{17}$ alloys. It is clear that $\Delta\rho/\rho_0$ of $(Fe\text{-}V)_{83}B_{17}$ decreases only monotonically as a function of x. This indicates that (i) there is no boundary T or scattering resonance in the spin-up $3d$ band of $(Fe\text{-}V)_{83}B_{17}$, or (ii) there is a possibility (Appendix B) that even though $\rho_{sd}^\uparrow$ has a resonance, $\Delta\rho/\rho_0$ may only decrease without a maximum due to the overdominance of ρ_{ss}. Since conclusion (ii) requires a few special assumptions, we prefer conclusion (i) as the explanation. Note, because the predicted x_T^a is located in the spin-glass phase region,[11] we think the resonance condition may also be affected by the spin-glass properties.

As in Fig 6, $\Delta\rho/\rho_0$ of $(Fe\text{-}V)_{83}B_{17}$ is 15–20 times smaller than that of Fe-V. When considering the relation between $\Delta\rho/\rho_0$ and magnetic moment (n_B), we see that while $\Delta\rho/\rho_0$ of Fe-V does not track its n_B for all x values, $\Delta\rho/\rho_0$ of $(Fe\text{-}V)_{83}B_{17}$ does.

IV. CONCLUSIONS

We have shown that experimental data of the magnetic moment, specific-heat coefficient, high-field susceptibility, residual resistivity, and anisotropic magnetoresistance of $Fe_{100-x}V_x$ and $(Fe_{100-x}V_x)_{83}B_{17}$ alloys. More evidences for the split-band model are given for the $Fe_{100-x}V_x$ alloys. However, there seems to be no definite conclusion about the applicability of the split-band and the charge-transfer models to the amorphous $(Fe_{100-x}V_x)_{83}B_{17}$ alloys. The similarities in the high-field susceptibility data between crystalline $Fe_{100-x}V_x$ and amorphous $(Fe_{100-x}V_x)_{83}B_{17}$ are encouraging. We have offered one explanation. Obviously, more studies are needed on these glassy materials.

ACKNOWLEDGMENTS

This work was supported by the National Science Council of ROC under Grant No. NSC 80-0208-M001-85. We are also thankful to Dr. Y. Y. Chen for the use of his low-temperature calorimeter, and to Dr. S. C. Jang and C. H. Tsau of ITRI for the use of their melt spinner.

APPENDIX A

In the spin-up d band, ϵ_F is almost near the top of the band. Hence, we may assume $D_\uparrow(\epsilon>\epsilon_F)$, the band-tail shape, to be linearlized,

$$\frac{D_\uparrow(\epsilon)}{D_\uparrow(\epsilon_F)}+\frac{\epsilon-\epsilon_F}{\Delta}=1\ , \tag{A1}$$

where $\epsilon=\epsilon_F+\Delta$ is at the band top;

$$D_\uparrow(\epsilon)=D_\uparrow(\epsilon_F)-\frac{D_\uparrow(\epsilon_F)}{\Delta}(\epsilon-\epsilon_F)\ ,$$
$$\left.\frac{dD_\uparrow(\epsilon)}{d\epsilon}\right|_{\epsilon=\epsilon_F}=-\frac{D_\uparrow(\epsilon_F)}{\Delta}<0\ . \tag{A2}$$

Since the number of holes in the spin-up band is

$$n_h^\uparrow=\int_{\epsilon_F}^{\epsilon_F+\Delta}D_\uparrow(\epsilon)d\epsilon\ , \tag{A3}$$

we find

$$n_h^\uparrow=\Delta\left[D_\uparrow(\epsilon_F)+\frac{1}{2}\left.\frac{dD_\uparrow}{d\epsilon}\right|_{\epsilon=\epsilon_F}\Delta\right]\ . \tag{A4}$$

If both $D_\uparrow(\epsilon_F)$ and $|dD_\uparrow/d\epsilon|$ are reduced, and $n_h^\uparrow$ is roughly constant ($\delta n_e^\uparrow$ is small, only 0.07), it is likely that Δ should increase. This is equivalent to state that the bandwidth is increased.

APPENDIX B

From Ref. 3, $\Delta\rho/\rho_0$ of amorphous materials can be generalized as

$$\Delta\rho/\rho_0\propto\frac{(\rho_{sd}^\downarrow-\rho_{sd}^\uparrow)(\rho_{sd}^\uparrow+\rho_{ss}^\uparrow-\rho_{sd}^\downarrow-\rho_{ss}^\downarrow)}{(\rho_{sd}^\uparrow+\rho_{ss}^\uparrow)(\rho_{sd}^\downarrow+\rho_{ss}^\downarrow)}\ . \tag{B1}$$

Since $\rho_{sd}^\uparrow\gg\rho_{sd}^\downarrow$, and $\rho_{ss}^\downarrow\simeq 120\ \mu\Omega\,\text{cm}\gg\rho_{sd}^\downarrow$,[3] Eq. (B1) is approximated as

$$\Delta\rho/\rho_0\propto\frac{\rho_{sd}^\uparrow(\rho_{sd}^\uparrow+\Delta\rho_{ss})}{\rho_{ss}^\downarrow(\rho_{sd}^\uparrow+\rho_{ss}^\uparrow)}\ , \tag{B2}$$

where $\rho_{ss}^\uparrow=\rho_{ss}^\downarrow+\Delta\rho_{ss}$. Here, $\rho_{sd}^\downarrow$ and $\rho_{sd}^\uparrow$ of $(Fe\text{-}V)_{83}B_{17}$ are the same as those of Fe-V, respectively. Then, we assume (i) $\rho_{ss}^\downarrow$ increases as ρ_0 increases, because $\rho^\uparrow=\rho_{ss}^\uparrow+\rho_{sd}^\uparrow\gg\rho_\downarrow=\rho_{ss}^\downarrow$ and $\rho_0\simeq\rho_{ss}^\downarrow$, (ii) $\rho_{sd}^\uparrow$ has a resonance, and increases from $x=0$ to $x=x_T^a$, (iii) $\rho^\uparrow$ is sa-

turated due to the lower limit of the electron mean free path.[24] Mathematically, the three assumptions are written as

$$\rho_{ss}^{\downarrow}=\rho_{ss}^{\downarrow}(x=0)+ax\ ,$$
$$\rho_{sd}^{\uparrow}=\rho_{sd}^{\uparrow}(x=0)+bx\quad(0<x<x_T^a)\ , \tag{B3}$$
$$\rho^{\uparrow}=\rho_{ss}^{\uparrow}+\rho_{sd}^{\uparrow}\simeq c\ ,$$

where a, b, and c are constants. After substituting Eq. (B3) into Eq. (B1), we have

$$\Delta\rho/\rho_0\propto\frac{[\rho_{sd}^{\uparrow}(x=0)+bx][c-\rho_{ss}^{\downarrow}(x=0)-ax]}{[\rho_{ss}^{\downarrow}(x=0)+ax]c}\ . \tag{B4}$$

Since the resonance is very weak, and the x dependence of $\rho_{ss}^{\downarrow}$ is about 2 $\mu\Omega$ cm/at. %, we take $[a/\rho_{ss}^{\downarrow}(x=0)]>[b/\rho_{sd}^{\uparrow}(x=0)]$. Also, $\rho_{sd}^{\uparrow}(x=0)>bx$ and $\rho_{ss}^{\downarrow}(x=0)>ax$ in general. After expanding Eq. (B4), it is easy to find that $\Delta\rho/\rho_0$ becomes a decreasing function of x. Thus, we have shown that even if $\rho_{sd}^{\uparrow}$ has a resonance, it is possible that $\Delta\rho/\rho_0$ may not have a maximum.

[1] L. Berger, Physica **91B**, 31 (1977).

[2] L. Berger, in *Evidence for split bands from electronic specific heat and electrical transport data in Fe-V and in other iron and nickel alloys,* edited by J. J. Becker and G. H. Lander, AIP Conf. Proc. No. 34 (AIP, New York, 1976), p. 355.

[3] A. P. Malozemoff, Phys. Rev. B **32**, 6080 (1985).

[4] S. N. Kaul and M. Rosenberg, Phys. Rev. B **27**, 5689 (1983).

[5] G. Böhnke, N. Croitoriu, M. Rosenberg, and M. Sostarich, IEEE Trans. Mag. **16**, 905 (1976).

[6] R. C. O'Handley, R. Hasegawa, R. Ray, and C. P. Chou, Appl. Phys. Lett. **29**, 330 (1976).

[7] K. Yamauchi and T. Mizoguchi, J. Phys. Soc. Jpn. **39**, 541 (1975); R. C. O'Handley and D. S. Boudreaux, Phys. Status Solidi A **45**, 607 (1978).

[8] R. C. O'Handley, Phys. Rev. B **18**, 2577 (1978).

[9] A. H. Morrish, *The Physical Principles of Magnetism* (Krieger, New York, 1980), p. 394.

[10] C. N. King, R. B. Zubeck, and R. L. Greene, in *Low Temperature Physics LT13,* edited by K. D. Timmerhaus, W. J. O'Sullivan, and E. F. Hammel (Plenum, New York, 1974), Vol. 4.

[11] U. Mizutani and M. Hasegawa, Physica B **149**, 267 (1988); W. Marshall, Phys. Rev. **118**, 1519 (1960).

[12] C. Kittel, *Introduction to Solid State Physics,* 5th ed. (Wiley, New York, 1976), p. 141.

[13] J. C. Slater, J. Appl. Phys. **8**, 385 (1937); L. Pauling, Phys. Rev. **54**, 899 (1938).

[14] M. Matsuura, T. Nomoto, F. Itoh, and K. Suzuki, Solid State Commun. **33**, 895 (1980); P. Höussler, G. Indlekofer, H. G. Boyen, P. Oelhafen, and H. J. Güntherdot, Europhys. Lett. **15**, 759 (1991).

[15] S. R. Nagel and T. Tauc, Phys. Rev. Lett. **35**, 380 (1975).

[16] N. Sueda and H. Fujiwara, J. Sci. Hiroshima Univ. A **35**, 59 (1971).

[17] M. Oliver, J. O. Strom-Olsen, and Z. Altounian, Phys. Rev. B **35**, 333 (1987).

[18] J. H. M. Stoelinga, R. Gersdorf, and G. de Vries, Physica **41**, 457 (1969).

[19] E. P. Wohlfarth, Phys. Lett. **3**, 17 (1962).

[20] R. Kubo and Y. Obata, J. Phys. Soc. Jpn. **11**, 547 (1956).

[21] A. M. Clogston, V. Jaccarino, and Y. Yafet, Phys. Rev. **134**, A650 (1964).

[22] L. Berger, Physica **30**, 1141 (1964).

[23] A. Fert and I. A. Campbell, Phys. Rev. Lett. **16**, 1190 (1968).

[24] Z. Fisk and G. W. Webb, Phys. Rev. Lett. **36**, 1084 (1976).